

# Lateral Diffusion of CO<sub>2</sub> in Leaves Is Not Sufficient to Support Photosynthesis<sup>[w]</sup>

James I.L. Morison<sup>1\*</sup>, Emily Gallouët<sup>1</sup>, Tracy Lawson, Gabriel Cornic, Raphaèle Herbin, and Neil R. Baker

Department of Biological Sciences, University of Essex, Colchester CO4 3SQ, United Kingdom (J.I.L.M., E.G., T.L., N.R.B.); Laboratoire d'Ecophysiologie Végétale, Université de Paris 11, 91405 Orsay, France (E.G., G.C.); and Laboratoire d'Analyse, Topologie, Probabilités, Université de Provence, 13453 Marseille, France (R.H.)

Lateral diffusion of CO<sub>2</sub> was investigated in photosynthesizing leaves with different anatomy by gas exchange and chlorophyll *a* fluorescence imaging using grease to block stomata. When one-half of the leaf surface of the heterobaric species *Helianthus annuus* was covered by 4-mm-diameter patches of grease, the response of net CO<sub>2</sub> assimilation rate (*A*) to intercellular CO<sub>2</sub> concentration (*C<sub>i</sub>*) indicated that higher ambient CO<sub>2</sub> concentrations (*C<sub>a</sub>*) caused only limited lateral diffusion into the greased areas. When single 4-mm patches were applied to leaves of heterobaric *Phaseolus vulgaris* and homobaric *Commelina communis*, chlorophyll *a* fluorescence images showed dramatic declines in the quantum efficiency of photosystem II electron transport (measured as *F<sub>q</sub>'*/*F<sub>m</sub>'*) across the patch, demonstrating that lateral CO<sub>2</sub> diffusion could not support *A*. The *F<sub>q</sub>'*/*F<sub>m</sub>'* values were used to compute images of *C<sub>i</sub>* across patches, and their dependence on *C<sub>a</sub>* was assessed. At high *C<sub>a</sub>*, the patch effect was less in *C. communis* than *P. vulgaris*. A finite-volume porous-medium model for assimilation rate and lateral CO<sub>2</sub> diffusion was developed to analyze the patch images. The model estimated that the effective lateral CO<sub>2</sub> diffusion coefficients inside *C. communis* and *P. vulgaris* leaves were 22% and 12% of that for free air, respectively. We conclude that, in the light, lateral CO<sub>2</sub> diffusion cannot support appreciable photosynthesis over distances of more than approximately 0.3 mm in normal leaves, irrespective of the presence or absence of bundle sheath extensions, because of the CO<sub>2</sub> assimilation by cells along the diffusion pathway.

Leaf CO<sub>2</sub> assimilation rates in C3 plants are sensitive to the intercellular CO<sub>2</sub> concentration (*C<sub>i</sub>*) primarily because of the poor affinity of Rubisco for CO<sub>2</sub> (e.g. Evans and von Caemmerer, 1996). The rate of diffusion of CO<sub>2</sub> into or out of the leaf depends on the partial pressure gradient and the resistance of the diffusion pathway from outside the leaf to the site of fixation, the chloroplasts. This pathway comprises the well-understood boundary layer and stomatal components and a less well-understood internal resistance, *r<sub>i</sub>* (for clarification of terminology, see Evans and von Caemmerer, 1996). Understanding *r<sub>i</sub>* is very important, as it determines the drop in CO<sub>2</sub> molar fraction between the substomatal space and the chloroplast, which is about 70 to 100 μmol mol<sup>-1</sup> (e.g. Parkhurst and Mott, 1990; Evans and Loreto, 2000; Singsaas et al., 2003). The value of *r<sub>i</sub>* is therefore critical to many aspects of photosynthetic modeling, for example, correct estimation of key photosynthetic model parameters (Parkhurst and Mott, 1990; Singsaas et al., 2003; Manter and Kerrigan, 2004; Warren 2004), assessment of the importance of carbonic anhydrase in chloroplastic CO<sub>2</sub> diffusion (e.g. Gillon and Yakir, 2000), and prediction of photosynthetic gains

from engineering C4 photosynthesis in C3 cells (von Caemmerer, 2003).

While numerous studies have attempted to determine *r<sub>i</sub>* in different species, there is as yet no complete model of it (Singsaas et al., 2003), and we need more information on its basis (Long and Bernacchi, 2003). The *r<sub>i</sub>* is the combination of an air space gaseous resistance, *r<sub>ias</sub>*, and a liquid phase resistance from the cell wall to the chloroplast, *r<sub>liq</sub>*. The air space diffusion resistance, *r<sub>ias</sub>*, should reflect the leaf structure, particularly the porosity, cell shape, and density of packing. At the scale of a few cells, *r<sub>ias</sub>* must be anisotropic, given the typical arrangement of packed vertical cylindrical cells in the palisade and more loosely arranged cells in the spongy mesophyll tissue (porosities in the two tissues are typically 15%–30% and 25%–65%, respectively; e.g. Terashima, 1992; Terashima et al., 1996). The *r<sub>ias</sub>* must also depend on the pathway, which is partly determined by the pattern of stomatal apertures. For example, if groups of stomata are closed in particular areas of the leaf, lateral CO<sub>2</sub> diffusion could become important (Terashima, 1992; Parkhurst, 1994), whereas homogeneous stomatal apertures result in CO<sub>2</sub> diffusion being predominately vertical over the small distance of the thickness of the leaf (or, for amphistomatous leaves, one-half of the thickness). At a larger scale of a few millimeters, in heterobaric leaves, bundle sheath extensions divide the leaf into numerous isolated gas compartments called areoles (Esau, 1977), and these extensions apparently restrict lateral CO<sub>2</sub> diffusion during photosynthesis. This is

<sup>1</sup> These authors contributed equally to the paper.

\* Corresponding author; e-mail morisj@essex.ac.uk; fax 44-1206-872592.

<sup>[w]</sup> The online version of this article contains Web-only data.

Article, publication date, and citation information can be found at [www.plantphysiol.org/cgi/doi/10.1104/pp.105.062950](http://www.plantphysiol.org/cgi/doi/10.1104/pp.105.062950).

suggested by the heterogeneous patterns of CO<sub>2</sub> assimilation observed in such leaves (e.g. Downton et al., 1988; Terashima et al., 1988). Therefore,  $r_{ias}$  is believed to be greater in heterobaric leaves compared with homobaric leaves in which these extensions are absent (Terashima et al., 1988; Parkhurst, 1994). Heterobaric leaf anatomy under certain conditions is associated with patchy stomatal behavior, which can be defined as stomata in "adjacent regions differing by exhibiting mean values that differ significantly" (p. 323; Weyers and Lawson, 1997). The importance of patchy stomatal behavior to net CO<sub>2</sub> assimilation rate ( $A$ ) and to the calculation of  $C_i$ , particularly during water stress, has been extensively debated (e.g. Terashima, 1992; Parkhurst, 1994). However, even when leaves are not "patchy," there can be significant spatial trends in stomatal aperture in both homobaric and heterobaric leaves so that lateral CO<sub>2</sub> diffusion could be important (Terashima et al., 1988; Weyers and Lawson, 1997).

There are rather few published empirical values for  $r_{ias}$  or its reciprocal, the air space conductance for CO<sub>2</sub>,  $g_{ias}$ . The upper limits to vertical  $g_{ias}$  can be estimated from the value of the diffusion coefficient of CO<sub>2</sub> ( $D_c$ ) in still air, and the overall mesophyll porosity and the leaf thickness. Taking ranges of values of the latter two parameters from the comprehensive survey of 56 species by Slaton and Smith (2002; e.g. 10%–30% porosity and 0.1–0.6 mm thickness) gives a  $g_{ias}$  range of 4.7 to 0.26 cm s<sup>-1</sup> (equivalent to molar conductances of 1.9–0.11 mol m<sup>-2</sup> s<sup>-1</sup>). Values measured have usually been at the lower end of this range (0.14–0.33 mol m<sup>-2</sup> s<sup>-1</sup>; Pieruschka et al., 2005). There are two possible factors causing these values: the tortuosity of the path length, which may reduce diffusion by 50% or more (Parkhurst and Mott, 1990; Syvertsen et al., 1995; Terashima et al., 1996), and the narrow diameter of the air spaces, causing more collision with cell walls (Leuning, 1983). There are even fewer estimates of lateral  $g_{ias}$ . Using respiration measurements, Pieruschka et al. (2005) recently determined much lower values that differ substantially between homobaric *Vicia faba* leaves (26 mmol m<sup>-2</sup> s<sup>-1</sup>) and heterobaric *Phaseolus vulgaris* leaves (0.3 mmol m<sup>-2</sup> s<sup>-1</sup>). However, it is difficult to determine what such  $g_{ias}$  values mean for two reasons. First, such conductance values are equal to the diffusion coefficient of the gas in air divided by the length of the path of diffusion, which is not precisely known and is likely to vary, particularly during patchy stomatal closure. Second, the basic conductance or resistance model breaks down when diffusion occurs in a medium with distributed sources or sinks (Parkhurst, 1994), and in the light the sinks vary markedly with  $C_i$  (particularly under CO<sub>2</sub> limiting conditions). It is therefore crucial to consider both the sink activity along the pathway and the physical limitation (resistance to diffusion determined by leaf anatomy) in determining intercellular diffusion rates (Parkhurst, 1994; Evans and von Caemmerer, 1996).

Parkhurst (1977) developed a three-dimensional (3-D) model of photosynthetic CO<sub>2</sub> uptake to estimate

$r_{ias}$  and concluded that intercellular diffusion is slow and thus can be an important factor limiting CO<sub>2</sub> assimilation rate (Parkhurst, 1977, 1994). However, Parkhurst's theoretical conclusions have had only limited experimental confirmation, as it has not been possible to measure CO<sub>2</sub> concentration profiles inside leaves and thereby estimate vertical or lateral diffusion and determine the effects of different anatomies and the effect of sink strength on CO<sub>2</sub> diffusion. In this work, we applied artificial patches of silicon grease to block stomata and examined the contribution of lateral diffusion using gas exchange. We also used the approach of Meyer and Genty (1998) combining gas exchange measurements and chlorophyll *a* fluorescence imaging to map the resulting two-dimensional (2-D) distribution of  $C_i$  across the leaf surface. In the patched area, diffusion through the stomata was eliminated; consequently, CO<sub>2</sub> supply for photosynthesis in the mesophyll under the patch was provided solely by lateral diffusion from the tissues surrounding the patch. Using this technique, it was possible to map  $C_i$  at a spatial resolution of 0.15 × 0.15 mm and study the lateral diffusion of CO<sub>2</sub> in leaves. We also developed a 2-D CO<sub>2</sub> diffusion model that included the activity of sinks along the pathway to estimate the effective lateral CO<sub>2</sub> diffusion coefficient,  $D_c'$ , from these data. We focused on two amphistomatous species with different leaf anatomy: *P. vulgaris*, a dicotyledonous species with heterobaric vein anatomy, and *Commelina communis*, a monocotyledonous, homobaric species. It is clear from the results that lateral diffusion over distances longer than 0.3 mm is not sufficient to provide for normal CO<sub>2</sub> assimilation rates in either of these two species and that vertical diffusion over short distances in normal conditions dominates CO<sub>2</sub> fluxes inside the leaf. The results also allay recent concerns that lateral diffusion through the leaf may cause errors in leaf photosynthetic measurements in small chambers (Long and Bernacchi, 2003).

## RESULTS

### Gas Exchange Demonstration of Limited Lateral Diffusion

When diffusion through the stomata was prevented by covering both sides of one-half of a leaf of sunflower (*Helianthus annuus*) with grease, the response of  $A$  to increasing ambient CO<sub>2</sub> concentration,  $C_a$ , showed that  $A$  was approximately halved (Fig. 1A). However, the shape was essentially the same as that for the leaf prior to covering, with the rate saturating at approximately the same  $C_a$ . Closer inspection shows that the ratio of  $A$  for the half-covered leaf ( $A^c$ ) to that for the complete leaf ( $A$ ) was slightly higher than one-half (0.53), which might indicate that some CO<sub>2</sub> did diffuse into the covered area to contribute to assimilation. However, this difference in ratio is equivalent to an additional 0.9-mm zone along the boundary

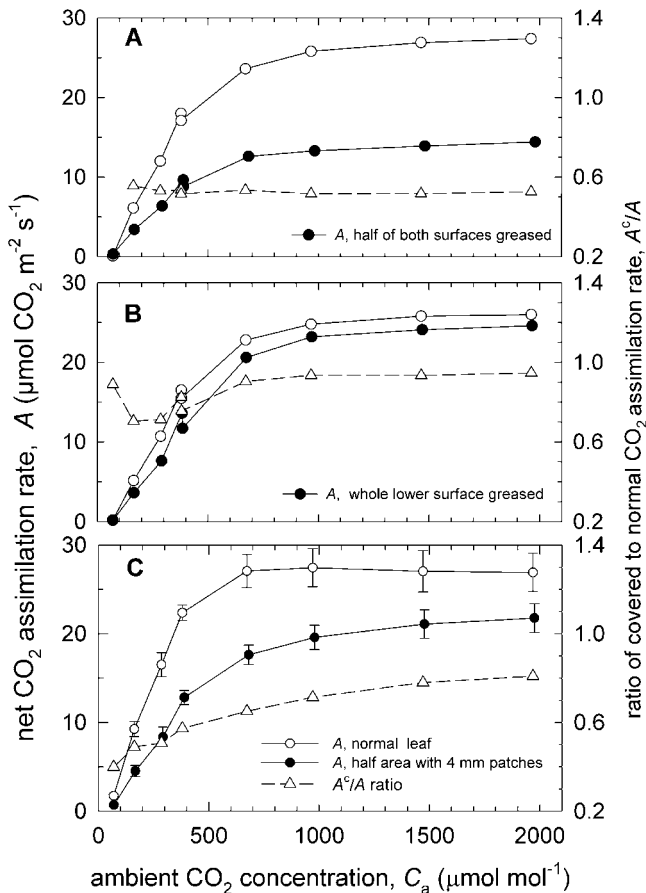


**Figure 1.** Response of net CO<sub>2</sub> assimilation rate,  $A$ , to increasing ambient CO<sub>2</sub> concentration,  $C_a$ , for sunflower leaves, with (●) and without (○) parts of the leaf being covered with grease. The right-hand axis (△) indicates the ratio of  $A$  in covered ( $A^c$ ) and not-covered ( $A$ ) leaves. A, One-half of the total leaf area covered (both surfaces; ●); B, the whole of the lower surface of the leaf covered (●); C, one-half of the leaf covered in 4-mm-diameter grease patches (both surfaces; ●). Conditions: PPFD = 1,000  $\mu\text{mol m}^{-2} \text{s}^{-1}$ ; leaf temperature = 25°C; water vapor in the leaf chamber approximately 15  $\text{mmol mol}^{-1}$ ;  $O_2 = 21\%$ .

between greased and untouched areas photosynthesizing at the full rate, which is within the accuracy of placement of the grease and chamber. The transpiration ratio  $T^c/T$  was very similar to the assimilation ratio (data not shown), showing that the grease was preventing diffusion through stomata and thereby affecting both CO<sub>2</sub> and H<sub>2</sub>O equally.

The substantial effect on the CO<sub>2</sub> assimilation rate of covering one-half of a leaf on both sides contrasts markedly with just covering the whole lower surface alone (Fig. 1, compare A and B). With the lower surface covered,  $A^c/A$  was only a minimum of 0.7, and more than 0.9 across most of the range of  $C_a$  from present atmospheric concentrations upwards. Sunflower leaves are amphistomatous, with typical ratios of lower to upper surface stomatal conductance of 1.7 (Morison, 1998), so that the upper surface stomata were able to supply CO<sub>2</sub>. Indeed, they opened slightly more, as the

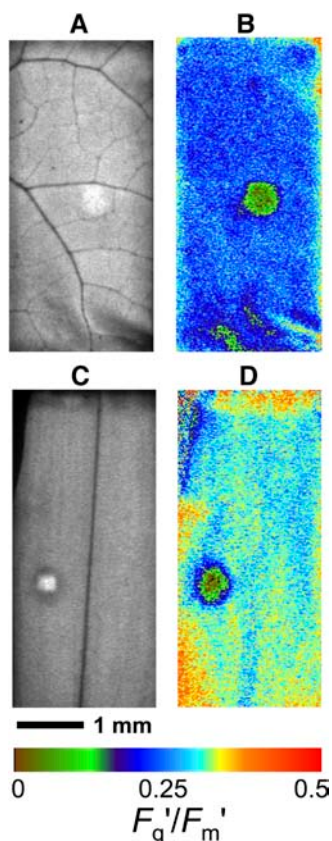
transpiration ratio  $T^c/T$  was approximately 0.6 over the whole  $C_a$  range. Therefore, the drop in calculated  $C_i$  was only 40  $\mu\text{mol mol}^{-1}$  (at  $C_a = 360 \mu\text{mol mol}^{-1}$ ). The  $A/C_i$  response was identical for normal leaves and those with the lower surface greased, showing that there was no effect of the treatment other than on the diffusion through stomata.

Figure 1A suggested that lateral diffusion across the short boundary (2 cm long) between greased and ungreased portions was slight. When a much larger boundary zone was created by covering approximately one-half of the leaf area with grease in small, 4-mm-diameter patches evenly distributed across the leaf surfaces, the  $A/C_i$  curve was markedly different (Fig. 1, compare C to A). Although  $A$  was approximately one-half at  $C_a = 370 \mu\text{mol mol}^{-1}$ , as  $C_a$  increased,  $A$  increased, showing no saturation, even up to  $C_a = 2,000 \mu\text{mol mol}^{-1}$ . The ratio  $A^c/A$  changed from 0.3 at 100  $\mu\text{mol mol}^{-1}$   $C_a$  to 0.81 at 2,000  $\mu\text{mol mol}^{-1}$ . However, transpiration was not affected by changing  $C_a$  as  $T^c/T$  remained close to 0.5 throughout, showing that it was not diffusion through the stomata that was changing with  $C_a$ . The changing ratio  $A^c/A$  therefore demonstrates that the higher  $C_a$  increased CO<sub>2</sub> diffusion laterally through the mesophyll. The effect produced a substantial increase in  $A$  because the distributed small patches provided a total perimeter length of 28 cm. However, even for this length perimeter, the additional photosynthesis at the highest  $C_a$  was equivalent to supplying CO<sub>2</sub> to a mesophyll zone only 0.6 mm wide photosynthesizing at the maximum rate.

### Chlorophyll Fluorescence Imaging

The CO<sub>2</sub> diffusion into patched areas of leaves was examined in detail with chlorophyll *a* fluorescence imaging. We contrasted the effect of the patch in the heterobaric *P. vulgaris* with the effect in the homobaric species *C. communis*. The imaging system clearly resolved in detail differences across the 10-cm<sup>2</sup> area of leaf enclosed, with vein patterns very evident in the steady-state fluorescence image  $F'$  (Fig. 2, A and C). The effect of a grease patch on the photosynthesis of the leaf was also clearly visible through  $F'$  and in the image constructed of  $F_q'/F_m'$  or the operating quantum efficiency of PSII electron transport (Fig. 2, B and D) in both *P. vulgaris* and *C. communis*.

When an image of  $F_q'/F_m'$  for a patch and surrounding region is viewed in more detail (Fig. 3A), it is striking that the  $F_q'/F_m'$  declines very steeply within a few pixels (<0.5 mm) of the edge of the patch and is <0.18 across a large area of the patch, with an approximate diameter of 2 mm. Note also that the  $F_q'/F_m'$  values in the area surrounding the patch are quite uniform (range 0.33–0.36). Using the calibration relationship determined prior to patching between whole image mean  $F_q'/F_m'$  and gas exchange-derived  $C_i$  (Fig. 11), we calculated  $C_i$  for each pixel after a patch was applied. The calculated  $C_i$  (Fig. 3B) in the middle



**Figure 2.** Images of chlorophyll fluorescence for 10-cm<sup>2</sup> leaf areas enclosed in a chamber (4.6 × 2.2 mm) during simultaneous gas exchange measurement. A and B are for *P. vulgaris*, and C and D are for *C. communis* leaves with a single 4-mm-diameter grease patch applied to both leaf surfaces. PPFD = 400 μmol m<sup>-2</sup> s<sup>-1</sup>; leaf temperature = 25°C; 1% O<sub>2</sub>; CO<sub>2</sub> = approximately 320 μmol mol<sup>-1</sup>. Images A and C are for *F'* (arbitrary gray scale). Images in B and D are for  $F_q'/F_m'$ , with the colored bar indicating how the range of values is mapped to the color palette; mean values are 0.239 and 0.300, respectively.

region of the patched area is very low, <50 μmol mol<sup>-1</sup>, and the gradient at the edge is approximately 320 μmol mol<sup>-1</sup> mm<sup>-1</sup>. The calculated image of *A* (Fig. 3C) essentially shows the same pattern as  $F_q'/F_m'$  (as suggested by the linear relationship between *A* and  $F_q'/F_m'$  in Fig. 11A), with a dramatic drop in photosynthesis in the patched area, and demonstrates that lateral diffusion of CO<sub>2</sub> was restricting photosynthesis.

Obviously if there is any lateral diffusion, the CO<sub>2</sub> molar fraction inside the patch and, consequently, *A* will depend on the molar fraction in the surrounding leaf (*C<sub>i</sub>*) and therefore on the *C<sub>a</sub>*. As *C<sub>a</sub>* is increased, *C<sub>i</sub>* outside the patch should increase, driving more lateral CO<sub>2</sub> diffusion. This effect is examined in Figures 4 and 5 for *P. vulgaris* and Figures 6 and 7 for *C. communis*. As expected,  $F_q'/F_m'$  in the unpatched area responded to *C<sub>i</sub>* (Fig. 4), increasing to 0.46 as *C<sub>i</sub>* was increased to >1,200 μmol mol<sup>-1</sup> and dropping to 0.18 at *C<sub>i</sub>* = 57 μmol mol<sup>-1</sup>. However, across this wide *C<sub>i</sub>* range, the effect of the patch is evident in all the images (Fig. 4), although the area of leaf affected by the patch

diminished as the adjacent *C<sub>i</sub>* increased, indicating some lateral diffusion. The *C<sub>i</sub>* values across the patches calculated from the  $F_q'/F_m'$  data are shown by the symbols in Figure 5 (the lines are modeled data; see later). Although the minimum *C<sub>i</sub>* in the middle of the patch increased slightly with increasing CO<sub>2</sub>, even at a *C<sub>i</sub>* of 1,270 μmol mol<sup>-1</sup> in the rest of the leaf, *C<sub>i</sub>* in the middle of the patch was as low as 40 μmol mol<sup>-1</sup> (Fig. 5B). In all cases, the patch affected a slightly larger area than the patch itself, presumably because there was no lateral CO<sub>2</sub> supply outward from the patched area. This effect is not so evident at the lowest *C<sub>i</sub>* because there is only a small lateral CO<sub>2</sub> gradient close to the CO<sub>2</sub> compensation molar fraction.

When patches were applied to *C. communis* leaves (Fig. 6), the *C<sub>i</sub>* concentrations in the surrounding leaf required to reduce the patch-affected area were considerably lower than in *P. vulgaris*. At the highest *C<sub>i</sub>* (1,375 μmol mol<sup>-1</sup>), blocking the stomata only affected  $F_q'/F_m'$  in an area about one-half of the patch diameter (Fig. 6D). The *C<sub>i</sub>* transect graphs (Fig. 7) showed that the minimum *C<sub>i</sub>* in the patch was <50 μmol mol<sup>-1</sup> for the three lowest CO<sub>2</sub> molar fractions, but at the highest *C<sub>i</sub>* of 1,375 it was 171 μmol mol<sup>-1</sup>.

Both of the species examined are amphistomatous, with similar leaf thicknesses and mesophyll sizes

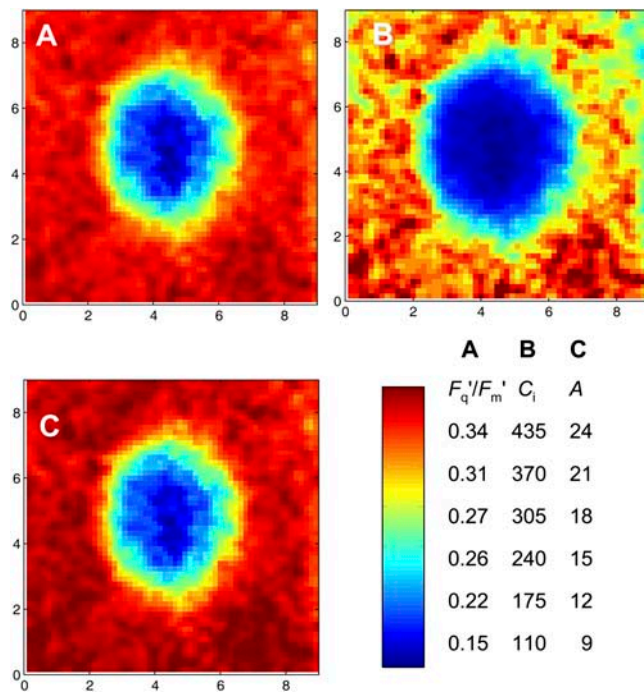


**Figure 3.** Effect of a 4-mm-diameter grease patch on photosynthesis in part of a leaf of *C. communis*. Grease was applied to both leaf surfaces. *C<sub>a</sub>* = 643 μmol mol<sup>-1</sup>; *C<sub>i</sub>* = 342 μmol mol<sup>-1</sup>; *g<sub>s</sub>* = 85 mmol m<sup>-2</sup> s<sup>-1</sup>; PPFD = 400 μmol m<sup>-2</sup> s<sup>-1</sup>. Axes shown are image scales in millimeters. Color bar is shown with relevant scales. A, Image of measured PSII efficiency ( $F_q'/F_m'$ ). B, Map of intercellular CO<sub>2</sub> concentration, *C<sub>i</sub>*, across the patch, calculated from A as described in "Materials and Methods." C, Map of net CO<sub>2</sub> assimilation rate, *A*, calculated from B.

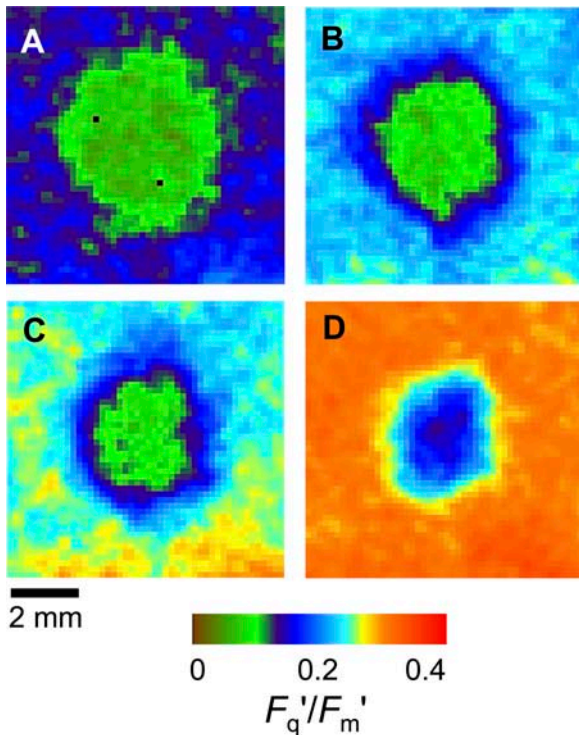


**Figure 4.** Images of PSII efficiency ( $F_q'/F_m'$ ) in part of a leaf of *P. vulgaris* (approximately  $8 \times 8$  mm) with a 4-mm-diameter grease patch applied to both sides at different external  $\text{CO}_2$  concentrations ( $C_a$ ). PPFD was  $400 \mu\text{mol m}^{-2} \text{s}^{-1}$ .  $C_a$  and intercellular  $\text{CO}_2$  concentration,  $C_i$ , values determined for the unpatched portion of the leaf were as follows: A,  $C_a = 97$ ,  $C_i = 57$ ; B,  $C_a = 270$ ,  $C_i = 166$ ; C,  $C_a = 360$ ,  $C_i = 227$ ; and D,  $C_a = 1,780$ ,  $C_i = 1,270 \mu\text{mol mol}^{-1}$ . The colored bar indicates how the range of  $F_q'/F_m'$  values is mapped to the color palette.

(Table I). However, both have much higher stomatal frequencies on the lower side than on the upper (Table I), as is usual in most herbaceous species, which consequently have typical conductance ratios of  $g_s^l/g_s^u \geq 2$ . Therefore, we hypothesized that patches on the upper surface alone would have less effect on  $F_q'/F_m'$  than patches applied to the underneath. This is confirmed by the images shown in Figure 8. For *P. vulgaris*, a patch on the upper surface (Fig. 8A) had only a small effect, both in the maximum drop in  $F_q'/F_m'$  and in the size of the area affected. At higher  $C_a$  (approximately  $900 \mu\text{mol mol}^{-1}$ ; data not shown), the effect on  $F_q'/F_m'$  of a patch on the upper surface alone could be almost eliminated. Note that the effect of both sides being patched (e.g. Fig. 4B) appears much more than the sum of the effect of the two sides singly; we believe this is caused by the compensation effect of the stomata opening further in the side that is not blocked, although we cannot quantify this from the gas exchange data that combines both surfaces. The limit to this effect is presumably reached at maximum stomatal aperture. In *C. communis*, there was almost no effect on  $F_q'/F_m'$  of patching the upper surface only (Fig. 8C), and this was the case at a range of  $C_a$  values (data not

shown). When the lower surface alone was patched, the effect was smaller than in *P. vulgaris*. It might be noted that the species difference in comparative patch effect between the two surfaces is contrary to the differences in stomatal frequency ratios (Table I, 5.0 compared to 3.4). However, what determines the severity of the  $C_i$  depletion when only one surface is patched is  $g_s$  of the remaining active surface, and previous measurements have shown that maximum  $g_s$  in *C. communis* is about twice that in *P. vulgaris* (Lawson et al., 1998a).

The resulting differences in  $C_i$  when upper or lower surfaces are patched are shown in Figure 9. The constant value across much of the patch when the lower surface was patched, even though not near the  $\text{CO}_2$  compensation concentration, indicates the supply of  $\text{CO}_2$  from the upper surface. For *P. vulgaris*, this

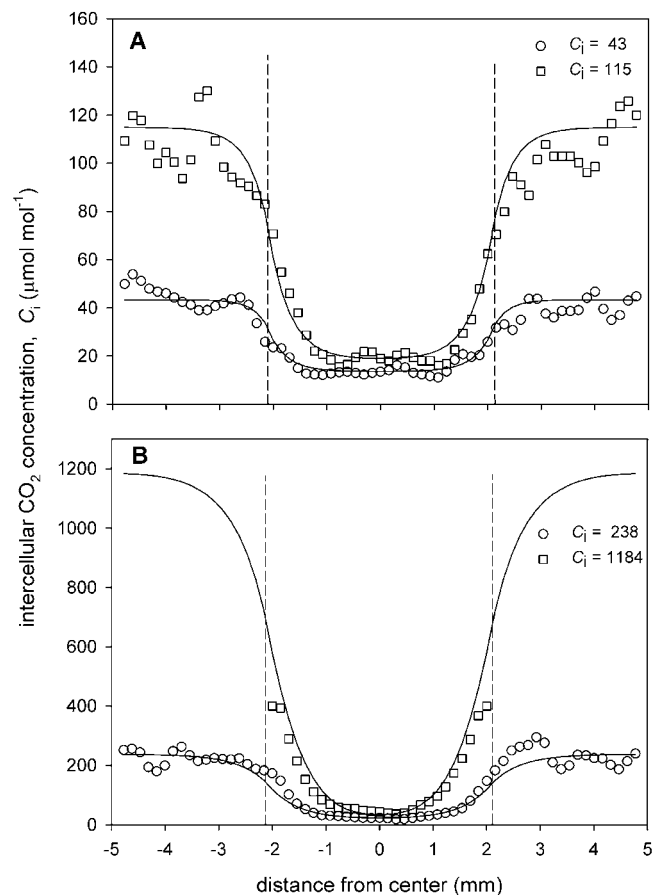


**Figure 5.** Transects of intercellular  $\text{CO}_2$  concentration,  $C_i$ , across a 4-mm-diameter grease patch applied to part of a leaf of *P. vulgaris*. Symbols indicate the mean  $C_i$  values calculated from the  $F_q'/F_m'$  images shown in Figure 4 for three rows of  $0.15 \times 0.15$ -mm pixels on a horizontal transect. Lines show the  $C_i$  values estimated from a model of lateral  $\text{CO}_2$  diffusion (see text for details). The fitted  $\text{CO}_2$  diffusion coefficient reduction factors,  $\phi$ , for the curves in A were 9.4% (lower) and 10.8% (upper), and in B were 15.8% (lower) and 8.5% (upper).  $C_i$  values shown are those for the unpatched leaf area. For the highest  $C_a$ ,  $C_i$  values above  $400 \mu\text{mol mol}^{-1}$  could not be reliably estimated from  $F_q'/F_m'$ . Dotted vertical lines indicate the position of the patch.

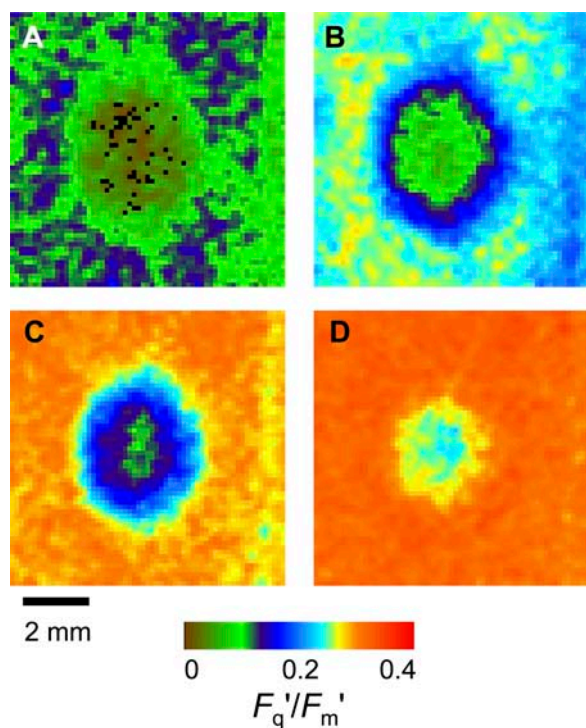


**Figure 6.** Images of PSII efficiency ( $F_q'/F_m'$ ) in part of a leaf of *C. communis* (approximately  $8 \times 8$  mm) with a 4-mm-diameter grease patch applied to both sides at different external CO<sub>2</sub> concentrations ( $C_a$ ). PPFD was  $400 \mu\text{mol m}^{-2} \text{s}^{-1}$ .  $C_a$  and intercellular CO<sub>2</sub> concentration,  $C_i$ , values determined for the unpatched portion of the leaf were as follows: A,  $C_a = 145$ ,  $C_i = 50$ ; B,  $C_a = 383$ ,  $C_i = 154$ ; C,  $C_a = 643$ ,  $C_i = 342$ ; and D,  $C_a = 1,790$ ,  $C_i = 1,375 \mu\text{mol mol}^{-1}$ . The colored bar indicates how the range of  $F_q'/F_m'$  values is mapped to the color palette.

minimum  $C_i$  value of  $40 \mu\text{mol mol}^{-1}$  can be compared directly with the value of  $15 \mu\text{mol mol}^{-1}$  observed in similar conditions when both surfaces were patched (Fig. 5A). For *C. communis*, the comparison is between 75 and  $21 \mu\text{mol mol}^{-1}$  (Fig. 7A). Although direct comparison of values between the species is not possible due to the different  $C_a$  used, the ratio of the minimum  $C_i$  in the patch to the  $C_i$  value in the surrounding leaf is a useful comparator: when the lower surface was patched, the ratio was substantially smaller for *P. vulgaris* than *C. communis* (0.33 and 0.44, respectively).

A 2-D photosynthesis and diffusion model was developed to analyze lateral CO<sub>2</sub> movement in patched leaves (Supplemental Appendix). The steeply changing values of  $C_i$  at the margins of the patch and the minimum value across much of the patch were accurately reproduced by the model. The root mean square relative error between model and estimated  $C_i$  values along horizontal transects across the patches, as exemplified in Figures 5 and 7, was typically  $<30\%$ , although at high  $C_a$  it was larger because  $C_i$  values  $>400 \mu\text{mol mol}^{-1}$  cannot be reliably determined from  $F_q'/F_m'$  due to saturation (Fig. 11A).

The key aspect of the model is the calculation of net photosynthetic CO<sub>2</sub> consumption along the diffusion

path because this is a major determinant of  $C_i$  as illustrated in Figure 10, A and B. When photosynthetic capacity is high (Fig. 10A), even if diffusion was as rapid as in free air in a 50% porosity medium (i.e. a diffusion reduction factor,  $\phi$ , of 50%), the model shows that a patch blocking stomata on both sides would cause pronounced depletion of  $C_i$  in the middle of the patch to  $70 \mu\text{mol mol}^{-1}$ , 30% of that calculated for adjacent leaf areas. This demonstrates the importance of the sink strength in determining CO<sub>2</sub> gradient under the patch. More realistically, mesophyll porosity is approximately 30% to 40% (see Table I and introduction), and the path length between closely packed, cylindrical cells must be more tortuous than in free air. Assuming that the path length is increased by  $\pi/2$  implies that the maximum  $D_c'$  inside a 35% porosity leaf should be about 22% of that in free air. Even at lower  $A$  rates,  $\phi$  of 20% would cause very large depletion (Fig. 10B). In our experiments, the  $A$  values at  $C_a = 360 \mu\text{mol mol}^{-1}$  were similar to, or a little lower

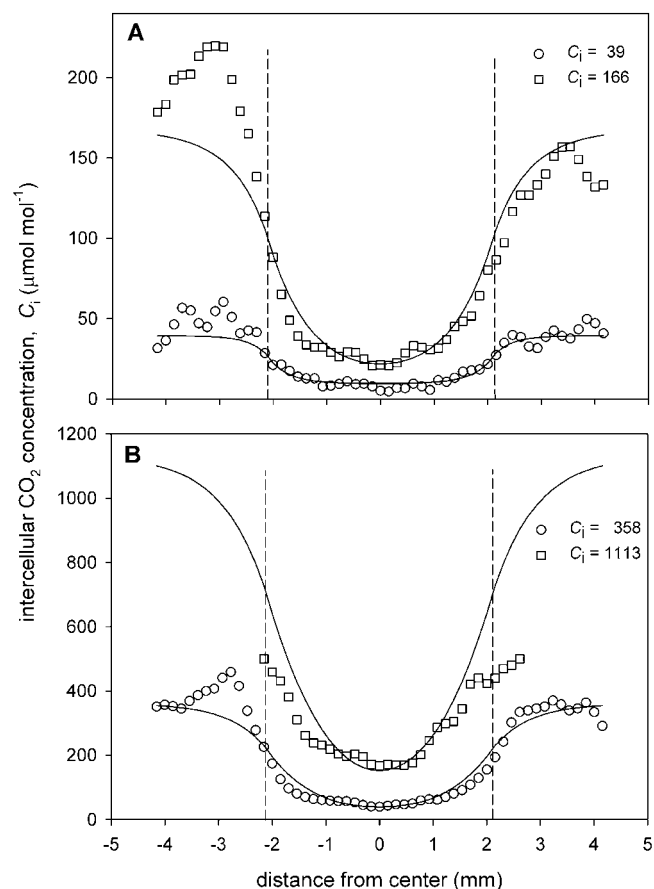


**Figure 7.** Transects of intercellular CO<sub>2</sub> concentration,  $C_i$ , across a 4-mm-diameter grease patch applied to part of a leaf of *C. communis*. Symbols indicate the mean  $C_i$  calculated from the  $F_q'/F_m'$  images shown in Figure 6. Lines show the  $C_i$  values estimated from a model of lateral CO<sub>2</sub> diffusion, with a fitted CO<sub>2</sub> diffusion coefficient reduction factor,  $\phi$ , of (A) 16.5% (lower) and 33.7% (upper), and (B) 25.5% (lower) and 23.2% (upper).  $C_i$  values shown are those for the unpatched leaf area. Other details are as in Figure 5.

**Table 1.** Anatomical characteristics of *P. vulgaris* and *C. communis* leaves used for the grease patch experiments

Measurements were taken on fully expanded primary *P. vulgaris* leaves and from main axis *C. communis* leaves. Leaf thickness and porosity were measured from leaf cross sections and stomatal density from leaf epidermal impressions. Means are of four leaves; SEs are shown in parentheses.

Measurement	<i>P. vulgaris</i>	<i>C. communis</i>
Leaf thickness ( $\mu\text{m}$ )	410 ( $\pm 33$ )	460 ( $\pm 30$ )
Tissue thickness ( $\mu\text{m}$ ) <sup>a</sup>		
Upper epidermis	31.6 ( $\pm 1.4$ )	54.9 ( $\pm 3.7$ )
Palisade	79.3 ( $\pm 4.4$ )	70.2 ( $\pm 2.2$ )
Spongy mesophyll	100.5 ( $\pm 2.8$ )	88.6 ( $\pm 7.9$ )
Lower epidermis	22.5 ( $\pm 2.8$ )	46.6 ( $\pm 1.4$ )
Porosity % <sup>b</sup>	36.4 ( $\pm 1.4$ )	40.9 ( $\pm 1.2$ )
Stomatal density ( $\text{mm}^{-2}$ )		
Upper leaf surface	21.3 ( $\pm 2.2$ )	13.6 ( $\pm 0.47$ )
Lower leaf surface	106.5 ( $\pm 6.4$ )	46.8 ( $\pm 2.2$ )
Lower/upper ratio	5.00	3.44

<sup>a</sup>Tissue thickness was measured on individual cells, so they sum to less than the leaf thickness measured on whole leaf sections. <sup>b</sup>Porosity was calculated as the percentage of the total leaf cross-sectional area of leaf comprising air spaces.

than, the higher rate case illustrated in Figure 10A. While there was some considerable variation in the values determined from the model for an individual patch image, for *C. communis* leaves the mean  $\phi$  was 22.0% and for *P. vulgaris* 12.4% (means of four and five leaves, respectively, estimated at a range of four to seven  $C_a$  values for each leaf; SEs of 2.7 and 1.8, means significantly different,  $P = 0.032$ , two-tailed  $t$  test). The small SEs for the  $\phi$  values reflect in part the variation between leaves but also suggest that the model provides a good description of diffusion in the leaf, given the widely different external  $\text{CO}_2$  conditions examined. Using the appropriate value for  $D_c$  (Supplemental Appendix), these  $\phi$  values correspond to  $\text{CO}_2$  diffusion coefficients of  $134 \mu\text{mol m}^{-1} \text{s}^{-1}$  for *C. communis* and  $73 \mu\text{mol m}^{-1} \text{s}^{-1}$  for *P. vulgaris*, which reflect differences in leaf anatomy between the two species.

The effect of changing  $C_a$  on the modeled  $C_i$  profile across a patch is shown in Figure 10C using  $\phi = 15\%$ , a value between those determined here for the two species. Clearly, even at high  $C_a$  ( $1,000 \mu\text{mol mol}^{-1}$ ), there is very large depletion in the patch, and the change in shape of the profiles is very similar to that evident in Figures 5 and 7.

## DISCUSSION

The gas exchange data with sunflower (Fig. 1) demonstrates that lateral diffusion of  $\text{CO}_2$  within a leaf is low: covering both sides of one-half of a leaf with grease caused a 50% decrease in net  $\text{CO}_2$  uptake, which remained essentially unchanged from  $C_a =$

$100 \mu\text{mol mol}^{-1}$  to  $C_a = 2,000 \mu\text{mol mol}^{-1}$ . Moreover, reducing the surface of a leaf by one-half by covering both sides with 4-mm-diameter patches of grease also caused a 50% decrease in  $A$  at  $C_a = 370 \mu\text{mol mol}^{-1}$ . But in this case the inhibitory effect of patches was progressively removed by increasing  $C_a$  (Fig. 1C), and extrapolation suggests that  $A$  of patched leaves would be the same as nonpatched leaves at  $C_a$  equals approximately  $7,000 \mu\text{mol mol}^{-1}$ . The much larger perimeter of the greased area when small patches were used therefore allowed enhanced diffusion of  $\text{CO}_2$  from the nonpatched to the patched area. This result recalls that of Terashima et al. (1988), who found that cutting *V. faba* leaf discs treated with abscisic acid into quarters restored the response of  $A$  to increased  $C_a$ , saturating at similar  $C_a$  values as found here. However, the difference is that sunflower is considered a heterobaric species while *V. faba* is homobaric and relatively porous (e.g. 53% porosity compared to 32% for *P. vulgaris* in the measurements of Pieruschka et al. [2005]). Indeed, both sunflower experiments showed that, at high  $C_a$ , large lateral  $\text{CO}_2$  gradients well in excess of

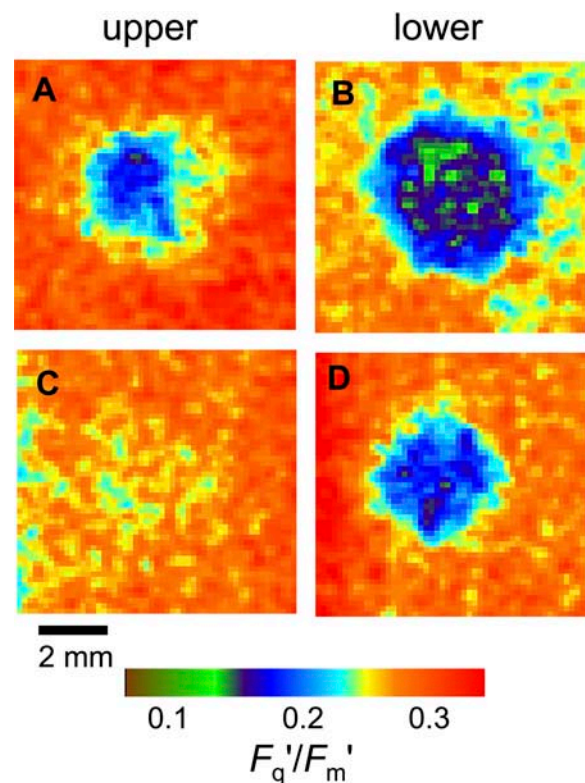


**Figure 8.** Images of PSII efficiency ( $F_q'/F_m'$ ) with 4-mm-diameter artificial grease patches applied to different leaf surfaces in *P. vulgaris* (A and B) and *C. communis* (C and D). Images approximately  $8 \times 8$  mm. PSII efficiency measured from upper surface with patch on upper surface only (A and C) or lower surface only (B and D).  $C_a$  and  $C_i$  values for the unpatched leaf from gas exchange measurements were as follows: A,  $C_a = 268$ ,  $C_i = 158$ ; B,  $C_a = 243$ ,  $C_i = 122$ ; C,  $C_a = 315$ ,  $C_i = 171$ ; and D,  $C_a = 315$ ,  $C_i = 171 \mu\text{mol mol}^{-1}$ . The colored bar indicates how the range of  $F_q'/F_m'$  values is mapped to the color palette.

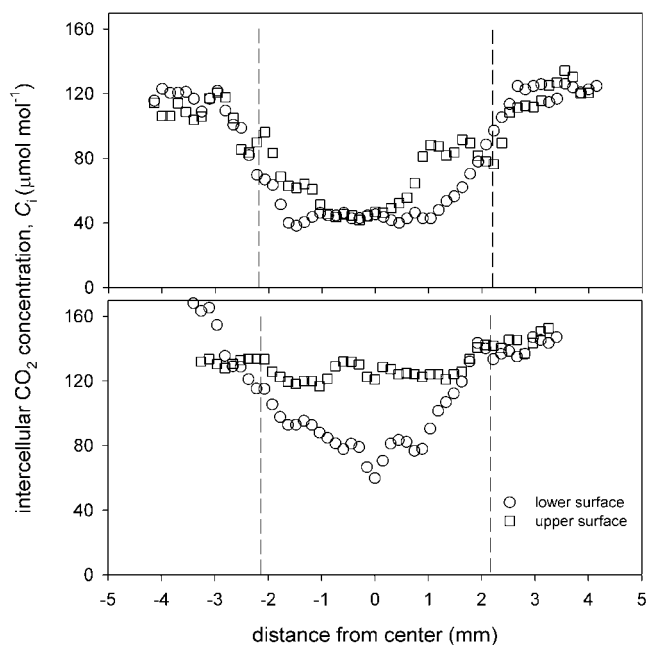


**Figure 9.** Transects of intercellular CO<sub>2</sub> concentration,  $C_i$ , across 4-mm-diameter patches applied to part of a leaf of *P. vulgaris* (top) or *C. communis* (bottom). Legend indicates whether patches applied to either upper or lower leaf surface only.

2,000  $\mu\text{mol mol}^{-1} \text{mm}^{-1}$  occurred between nonpatched and patched areas, suggesting high resistances to lateral diffusion.

Imaging the PSII efficiency ( $F_q'/F_m'$ ) of the mesophyll when stomata were blocked with grease patches allowed us to assess lateral CO<sub>2</sub> diffusion in photosynthesizing leaves, over distances determined by the image pixel size of  $0.15 \times 0.15$  mm. The images of the drop in  $F_q'/F_m'$  underneath artificial patches shown in Figures 2 to 4 and 8 are striking. As there was a linear relationship between  $A$  and  $F_q'/F_m'$  in our experimental conditions (Fig. 11B), the sharp declines in  $F_q'/F_m'$  at the edges of patches demonstrate that there was not sufficient lateral CO<sub>2</sub> diffusion over distances of more than 0.3 to 0.5 mm to support substantial photosynthesis in either *C. communis* or *P. vulgaris*, agreeing with the gas exchange data for sunflower. Furthermore, we used the relationship between mean  $F_q'/F_m'$  and mean  $C_i$  to calculate pixel values of  $C_i$  under patches. These showed that there were large lateral gradients in  $C_i$  across a patch margin ( $>250 \mu\text{mol mol}^{-1} \text{mm}^{-1}$  at normal  $C_a$ , much larger at high  $C_a$ ). These lateral gradients are considerably larger than the vertical gradients across leaves of approximately  $100 \mu\text{mol mol}^{-1} \text{mm}^{-1}$ , given by Terashima (1992) and Parkhurst et al. (1988). Furthermore, while lateral diffusion was clearly more effective in the homobaric *C. communis* than in the heterobaric *P. vulgaris*, lateral fluxes were still very low. Images of grease patches applied to two other species, tobacco (*Nicotiana tabacum*) and sunflower (homobaric and heterobaric, respectively), showed the same severe inhibition of  $A$  (data

not shown). We conclude that even if bundle sheath extensions are absent, lateral CO<sub>2</sub> diffusion at these spatial scales (representing between five and 25 mesophyll cells) is insufficient for appreciable photosynthesis at normal  $C_a$ . Obviously, mesophyll cell packing will affect the speed of lateral diffusion and photosynthetic rate will affect the  $C_i$  depletion. Therefore, it is likely that there would be a difference in  $D_c'$  between palisade and spongy mesophyll tissues (Parkhurst, 1986; Terashima, 1992). The fluorescence measurements were only from the upper leaf surface and, therefore, primarily of the palisade tissue. However, as blocking stomata reduced  $F_q'/F_m'$  in the palisade, it is clear that lateral diffusion in the leaf as a whole is slow enough to restrict photosynthesis, and

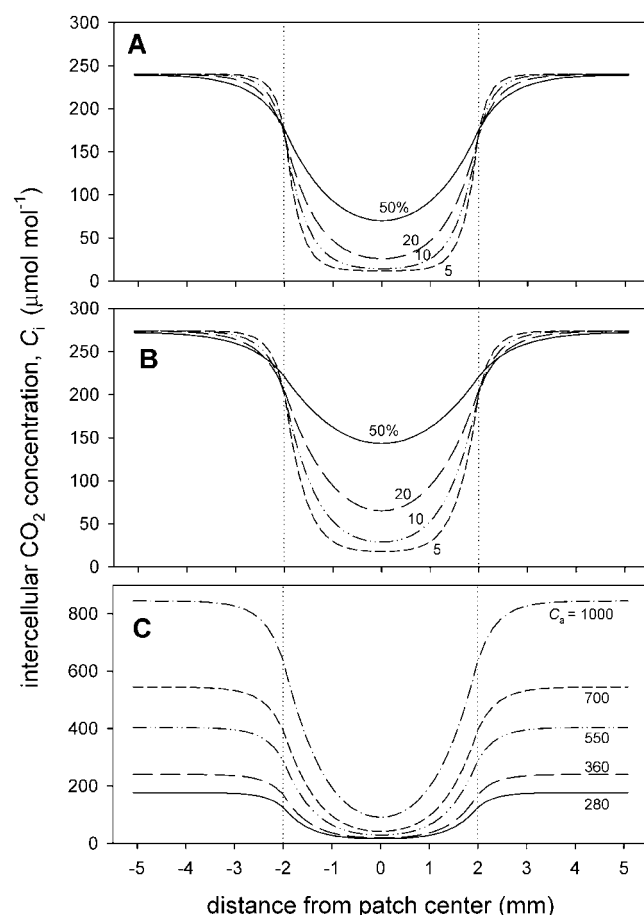


**Figure 10.** Transects of intercellular CO<sub>2</sub> concentration,  $C_i$ , across a 4-mm-diameter patch (limits indicated by dotted vertical lines) calculated from the diffusion model. A and B show results for different reduction factor values,  $\phi$ , for the CO<sub>2</sub> diffusion coefficient  $D_c$  at fixed  $C_a$  (360  $\mu\text{mol mol}^{-1}$ ) and either high (A) or low (B) net CO<sub>2</sub> assimilation capacities (as indicated by the rate outside the patch of 23.5 and 12.1  $\mu\text{mol m}^{-2} \text{s}^{-1}$ , respectively). Numbers indicate  $\phi$  in percentages. Model parameters were as follows: A,  $g_s^c = 200 \text{ mmol m}^{-2} \text{s}^{-1}$ , leaf thickness = 400  $\mu\text{m}$ ,  $a = 45 \mu\text{mol m}^{-2} \text{s}^{-1}$ ,  $b = 160 \mu\text{mol mol}^{-1}$ ,  $c = 3.0 \mu\text{mol m}^{-2} \text{s}^{-1}$ ; and B,  $g_s^c = 140 \text{ mmol m}^{-2} \text{s}^{-1}$ ,  $a = 20 \mu\text{mol m}^{-2} \text{s}^{-1}$ ,  $b = 90 \mu\text{mol mol}^{-1}$ ,  $c = 3.0 \mu\text{mol m}^{-2} \text{s}^{-1}$  (see "Materials and Methods"). C shows  $C_i$  values for different  $C_a$ , using parameters from the high A case in A, with  $\phi = 15\%$ ;  $C_a$  values are indicated.

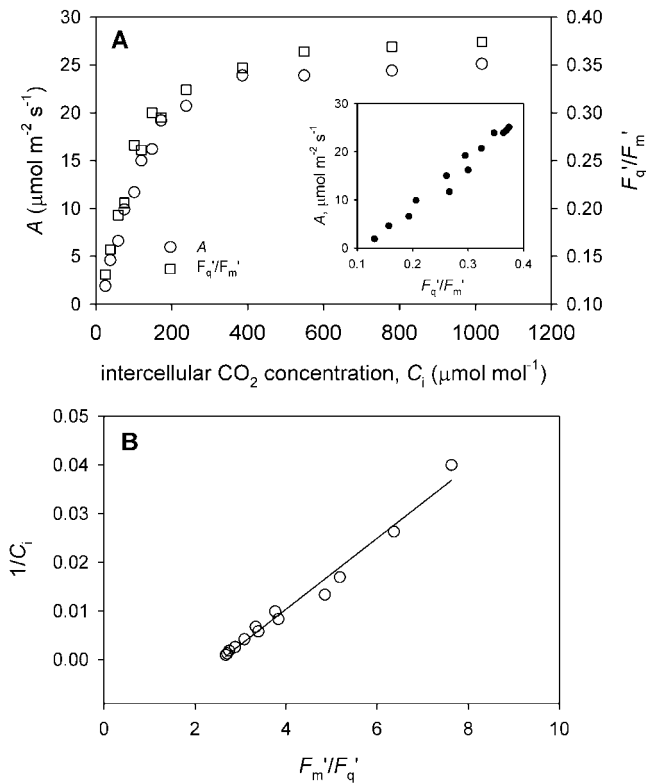


**Figure 11.** A, Example calibration information: relationships between net CO<sub>2</sub> assimilation rate ( $A$ ),  $F_q'/F_m'$  (PSII quantum efficiency), and intercellular CO<sub>2</sub> concentration ( $C_i$ ) for *P. vulgaris*. PPFD 400  $\mu\text{mol m}^{-2} \text{s}^{-1}$ ; leaf temperature = 25°C; 1% O<sub>2</sub>. Insert graph in A is data replotted as  $A$  versus  $F_q'/F_m'$ . B, Data from A replotted as the double reciprocal plot,  $1/C_i$  against  $F_m'/F_q'$ .

the spongy tissue does not therefore act as an effective high permeability CO<sub>2</sub> supply route for the palisade, as has been suggested (Parkhurst, 1986).

Our results suggest that the internal air space resistance,  $r_{ias}$ , between substomatal cavity and mesophyll is dominated by the vertical pathway, and lateral diffusion plays little part. Indeed, both the sunflower data (Fig. 1) where there was minimal effect on  $A$  when the stomata in one surface were blocked and the image in Figure 8C for *C. communis* when the upper surface only was blocked demonstrate that vertical diffusion over the thickness of the leaf is clearly effective. This is obviously a result of the vertical orientation of palisade mesophyll cells and the dense spacing of stomata. Leaves are usually thin, typically 0.2 to 1.0 mm thick, and we should expect that diffusion over longer distances is a limitation, particularly laterally.

It should be noted that we used only moderate light intensity for these experiments with *C. communis* or *P. vulgaris* to have sufficient sensitivity in the response of  $F_q'/F_m'$  to CO<sub>2</sub> (Fig. 11A). Although the  $A$  rates were moderate, at higher light intensity the much larger CO<sub>2</sub> sinks would mean an even steeper gradient of CO<sub>2</sub> across patch perimeters. However, in normal O<sub>2</sub> concentrations, photorespiration would reduce the CO<sub>2</sub> depletion so that the minimum values would

presumably only drop as low as 50 to 100  $\mu\text{mol mol}^{-1}$ , i.e. close to the normal compensation CO<sub>2</sub> molar fraction. A second point is that our calculated images of  $C_i$  are derived from gas exchange measurements, so the  $C_i$  value is actually the mean substomatal CO<sub>2</sub> concentration. It is this that we have modeled. As pointed out in several articles (e.g. Terashima et al., 2001), the CO<sub>2</sub> concentration within the mesophyll air spaces in photosynthesizing leaves is lower than the substomatal concentration, although the effect is likely to be least in thin, amphistomatous leaves as examined here. The  $F_q'/F_m'$  measurements are those from the upper mesophyll cells and the stomatal conductance in these leaves is usually substantially lower on the upper surface, so in the unpatched areas of leaf we may be slightly overestimating the CO<sub>2</sub> concentration close to the imaged mesophyll. The overestimation depends on vertical diffusion, and the actual  $C_i$  in the intercellular air spaces is likely to be 10 to 20  $\mu\text{mol mol}^{-1}$  lower than the measured  $C_i$  (e.g. Parkhurst and Mott, 1990; Evans and Loreto, 2000; Singaas et al., 2003).

The modeling analysis suggests that the effective lateral CO<sub>2</sub> diffusion coefficient inside the leaves ( $D_c'$ ) is approximately 10% to 25% of that for free air. While this is in the range expected from typical values of mesophyll porosity (see introduction) and the likely increase in path-length tortuosity, there are some uncertainties in the exact  $D_c'$  values. First, the model estimates are very sensitive to the physical patch size, which is difficult to determine exactly as it spreads out slightly during application. Second, estimates of  $D_c'$  also depend slightly on the stomatal conductance values used, and in some cases  $C_i$  values estimated from the model for areas outside the patch overestimated those derived from gas exchange for the whole leaf area in the chamber. This is probably caused by heterogeneity in conductance across the leaf. Third, the  $C_i$  profiles are sensitive to the parameters of the  $A/C_i$  relationship but relatively insensitive to the  $\phi$  value (Fig. 10, compare A and B). Nevertheless, we found higher values of  $\phi$  in leaves of *C. communis* than in *P. vulgaris* (22% and 12% of that in free air, respectively), reflecting anatomical differences. These two species are usually classified as homobaric and heterobaric, respectively. However, in view of their many anatomical differences as monocot and dicot species, it is simplistic to attribute the differences in  $D_c'$  to the presence or absence of bundle sheath extensions, especially as no species is completely homobaric because primary veins exhibit bundle sheath extensions (Weyers and Lawson, 1997). Similarly, several articles have attempted to relate diffusion resistances to various measures of the air space porosity inside leaves. Here, measurements on transverse sections did not show any significant differences in porosity between the species (Table I). In addition, it is noticeable that while the  $F_q'/F_m'$  images in Figures 2 to 4 and 6 show the patch effect to be circular in the dicot *P. vulgaris*, those for *C. communis* are slightly elongated in the vertical

direction (parallel to the leaf length and corresponding to the venation direction). This suggests that there is a difference in  $D_c'$  depending on the direction of diffusion. Obviously  $D_c'$  is determined by permeability and not porosity alone, which would require a full assessment of air space volume and the volume of air spaces and their connectivity from transverse, longitudinal, and paradermal sections.

There have been suggestions recently that lateral diffusion of CO<sub>2</sub> in leaves can be sufficient to cause errors in gas exchange measurements because of gases external to the chamber diffusing through the clamped leaf into the chamber (Jahnke and Krewitt, 2002; Pons and Welschen, 2002; Long and Bernacchi, 2003). For example, Jahnke and Krewitt (2002) found an effect of the CO<sub>2</sub> concentration outside the chamber on the respiration of mature tobacco leaves. The chamber Jahnke and Krewitt used had an 8-mm-wide gasket, so the observed effect implies a high  $D_c'$ , which would affect many chamber systems (e.g. the LI-COR 6400 standard chamber has a gasket width of 6 mm). However, their measurements were done with high CO<sub>2</sub> gradients in respiring tissue. In illuminated leaves, as our results show, CO<sub>2</sub> assimilation by cells along the pathway depletes the CO<sub>2</sub> so that diffusion over more than a few tenths of a millimeter is ineffective. Indeed, the data of Pons and Welschen (2002), which showed that light saturated rates of photosynthesis in leaves of homobaric *Plantago major* were not affected by chamber perimeter length while respiration was, confirms this point. Therefore, the images in Figures 4 and 6 should restore confidence in gas exchange measurement of moderate photosynthetic rates with small chambers with large perimeter to area ratios. It is more likely that leakage at the leaf/gasket interface and difficulties in illumination conditions around the edge of chambers are potential problems for such chambers.

Recently, values for lateral  $g_{ias}$  have been determined by Pieruschka et al. (2005) using respiration measurements, and they showed marked differences between homobaric (*V. faba* and tobacco) and heterobaric (*P. vulgaris* and *Glycine max*) leaves. We have not used our data to estimate  $g_{ias}$  because of the inherent problems with the conductance model when considering diffusion in a system with sinks and sources (see introduction and Parkhurst [1994]). Instead, we prefer to characterize the diffusivity within leaves by  $\phi$  (the ratio of the diffusion coefficient for CO<sub>2</sub> inside the leaf,  $D_c'$ , to that for free air,  $D_c$ ), derived from a diffusion model. Pieruschka et al. (2005) calculated  $D_c'$  from their measurements of  $g_{ias}$  and the diffusion pathway length in respiring leaves. For the two homobaric species they examined, tobacco and *V. faba*,  $D_c'$  was approximately 75 and 200  $\mu\text{mol m}^{-1} \text{s}^{-1}$ , respectively. The  $\phi$  value of 22% for *C. communis* measured here produces a comparable diffusion coefficient value of 134  $\mu\text{mol m}^{-1} \text{s}^{-1}$ . However, the  $\phi$  value of 12% for the heterobaric *P. vulgaris* here corresponds to 73  $\mu\text{mol m}^{-1} \text{s}^{-1}$ , which is much higher than their estimate of approximately 2  $\mu\text{mol m}^{-1} \text{s}^{-1}$ . Pieruschka et al.

(2005) indicate that these low diffusivities were at the limit of their measurement accuracy; in addition, their analysis approach does not allow for sinks or sources of CO<sub>2</sub> in the pathway.

The need to include sinks and sources has previously led to the development of several diffusion models for leaves, and Parkhurst made a major contribution (e.g. Parkhurst, 1977). Parkhurst and Mott (1990) developed Parkhurst's original 3-D model to describe the effect of gas mixtures on intercellular CO<sub>2</sub> diffusion. A 3-D model could be adapted for the analysis of the artificial "patch" results. However, such a model would be highly dependent on the nonlinear response of  $A$  to  $C_i$  (the source term in the model), which will vary with light penetration and between different cell types. As we do not have any experimental data on the variation of light and photosynthetic characteristics with depth in the leaves examined here, nor the detailed anatomical information required to estimate vertical variation in  $D_c'$ , we would have to make assumptions and fit the required parameters with the model. The considerable uncertainties that would result are not merited since our main objective is characterization of lateral diffusion. We used a 2-D model that averages  $A$  and  $C_i$  through the leaf thickness, which is obtained by integrating the 3-D diffusion equation over the leaf depth (see Gallouët and Herbin [2005] for details). There are, of course, some drawbacks in using the 2-D model instead of the 3-D implementation (Gallouët and Herbin, 2005), and the depth-averaged model cannot give any quantitative information on the vertical diffusion. Interestingly, the Parkhurst and Mott (1990) 3-D model simulated measured  $A$  responses well when they used an effective diffusion reduction factor,  $\phi$  of 25%, similar to the 22% value that we found fit our observations for *C. communis*. This gives some confidence in the validity of the different modeling approaches used here and by Parkhurst. Other leaf diffusion models have been developed, but they have been for very small leaf slices with a single stoma or a few stomata, (e.g. Pachepsky and Acock, 1996), or have found that lateral diffusion is very small compared to vertical diffusion on the small lateral scales considered (e.g. Aalto and Juurola, 2002).

Finally, we have shown that application of grease at similar scales to those of natural patches (Lawson et al., 1998b) produces "patches" of  $A$  even in homobaric leaves. Indeed, Terashima et al. (1988) previously showed some patchy starch formation in the homobaric *V. faba*, although it was less marked than in sunflower (for review of other examples for homobaric leaves, see Terashima, 1992). We have not determined  $D_c'$  for a species as porous as *V. faba*; however, the model calculations in Figure 10 show that closed stomata will substantially reduce photosynthesis even if  $D_c'$  is as high as 50% of that for free air. Such a high  $D_c'$  is clearly unlikely. Therefore, these natural and artificial examples of patchiness of  $A$  demonstrate that it is patchy stomatal apertures that determine if  $A$  heterogeneity occurs, not differences in lateral CO<sub>2</sub> diffusion, as is often inferred (e.g. Syvertsen et al., 1995;

Evans and von Caemmerer, 1996). This suggests to us that the key difference between homobaric and heterobaric leaves is that in heterobaric leaves the areoles are isolated hydraulically and thus can show patchy stomatal behavior (Mott et al., 1999), whereas in homobaric leaves the stomata are not hydraulically isolated and show more gradual trends in stomatal aperture (Weyers and Lawson, 1997).

## CONCLUSION

Our results confirm for lateral CO<sub>2</sub> diffusion the theoretical calculations and suggestions of Parkhurst (1977, 1994) that intercellular diffusion in leaves is slow and thus can limit CO<sub>2</sub> assimilation rate. Both gas exchange data and  $F_q'/F_m'$  images of patched leaves lead us to conclude that, in the light, lateral CO<sub>2</sub> diffusion cannot support appreciable photosynthesis over distances of more than 0.2 to 0.5 mm in normal leaves. Although there are differences in the lateral diffusivity between leaves with different anatomy, if stomata are blocked or closed in actively photosynthesizing leaves, the CO<sub>2</sub> assimilation by cells along the diffusion pathway prevents significant lateral CO<sub>2</sub> transfer.

## MATERIALS AND METHODS

### Plant Material

Seeds of *Commelina communis* (originally supplied by Lancaster University), sunflower (*Helianthus annuus* L. cv LG53.80M; LG Seeds), and *Phaseolus vulgaris* L. cv Vilbel (Nickerson Seeds) were sown in a peat and loam-based compost (F2; Levington Horticulture) and grown in a heated glasshouse. Measurements were made on attached fully expanded primary leaves of *P. vulgaris* plants that were 3 to 4 weeks old and on the youngest fully expanded leaves of *C. communis* and sunflower plants that were 5 to 6 weeks old. Temperature was maintained above 20°C at night and rarely exceeded 30°C during the day. The plants were well watered throughout. Supplemental lighting (350  $\mu\text{mol m}^{-2} \text{s}^{-1}$ ) was provided from 07 h to 19 h by sodium vapor lights.

### A/C<sub>i</sub> Measurements with One-Half of the Leaf Covered

Responses of *A* to internal CO<sub>2</sub> concentration (*A/C<sub>i</sub>* curves) were measured for leaves of sunflower using a portable gas exchange system (Li-6400 [LI-COR] with standard leaf chamber and red and blue LED light source). Initially leaves were allowed to stabilize for approximately 30 min to the leaf chamber conditions, where CO<sub>2</sub> was maintained at 400  $\mu\text{mol mol}^{-1}$ , 21% O<sub>2</sub>, leaf temperature of 25°C, photosynthetic photon flux density (PPFD) of 1,000  $\mu\text{mol m}^{-2} \text{s}^{-1}$ , and water vapor pressure difference of  $1.1 \pm 0.2$  kPa. After stabilization, an *A/C<sub>i</sub>* curve was constructed by first decreasing and then increasing the chamber CO<sub>2</sub> concentration (*C<sub>a</sub>*). Then one-half of the leaf area (both surfaces) was covered with grease (High Vacuum; BDH), either as one contiguous block from the midline of the leaf area in the chamber or in 20 4-mm-diameter patches applied to the leaf. The leaf was placed back in the chamber in an identical position and allowed to stabilize for approximately 30 min. After stabilization, a second *A/C<sub>i</sub>* curve was constructed, identical to that described above.

### Chlorophyll *a* Fluorescence Imaging with Single Patches

Images of chlorophyll *a* fluorescence were obtained on attached leaves, essentially as described by Barbagallo et al. (2003), using a CF Imager (Technologica), with a spatial resolution of approximately  $0.15 \times 0.15$  mm. The orange LEDs in the imaging system (output spectra 580–700 nm, peak wavelength 648 nm) provided a PPFD of 400  $\mu\text{mol m}^{-2} \text{s}^{-1}$ . Steady-state

fluorescence (*F'*) was continuously monitored, while maximum fluorescence in the actinic light (*F<sub>m</sub>'*) was measured during an 800-ms exposure to a saturating pulse of 4,800  $\mu\text{mol m}^{-2} \text{s}^{-1}$ . Using the images captured at *F'* and *F<sub>m</sub>'*, images of PSII photosynthetic efficiency ( $F_q'/F_m' = (F_m' - F')/F_m'$ ) were constructed by the imaging software. Simultaneous measurements of gas exchange were taken using a 10-cm<sup>2</sup> area stirred leaf chamber [model PLC(B); PP Systems] with a low reflectance window (Edmund Optics) attached to a portable infrared gas analysis system (CIRAS1; PP Systems). Leaves were illuminated and imaged from above. Leaves were placed in the chamber and allowed to stabilize for at least 30 min to the chamber conditions, which were CO<sub>2</sub> molar fraction of 370  $\mu\text{mol mol}^{-1}$ , water vapor pressure of approximately 1.8 kPa, and leaf temperature of 24°C to 27°C giving leaf-air vapor pressure differences in the range 0.7 to 1.4 kPa. Oxygen concentration was maintained at 1% throughout by supplying air from a cylinder of 1% oxygen in nitrogen (BOC Gases). Gas exchange measurements were recorded just before the saturating pulse was applied. On each leaf measured, a calibration curve was constructed first as described below. Then a single patch 4 mm in diameter was applied to the adaxial, abaxial, or both leaf surfaces as required using neoprene foam discs cut to the appropriate size with cork borers, mounted onto forceps, and evenly covered with silicon grease. The leaves were again allowed to stabilize to the chamber conditions, and images and gas exchange measurements were then taken at various *C<sub>a</sub>* when assimilation rate was stable. As a single 4-mm-diameter patch represented only 1.3% of the area of the leaf in the chamber, we assumed that the gas exchange values accurately reflected the conditions in the unpatched area of the leaf. Using ungreased discs, we verified that the pressure applied during patching did not show any subsequent damage effects in fluorescence images, and we verified that the grease alone had no effect on dark-adapted PSII efficiency.

### Treatment of Data

To determine the relationship between PSII quantum efficiency ( $F_q'/F_m'$ ) and *C<sub>i</sub>*, gas exchange measurements were recorded simultaneously with chlorophyll fluorescence on leaves without patches at varying external CO<sub>2</sub> concentration and 1% O<sub>2</sub> concentration. The PSII quantum efficiency was averaged across the image, and variations were typically small (see Fig. 2 for examples). The example in Figure 11A illustrates that as photorespiration was suppressed at this low O<sub>2</sub> concentration, both *A* and  $F_q'/F_m'$  were very similarly shaped saturation functions of *C<sub>i</sub>* and linearly related (inset graph). In these conditions, a double reciprocal plot between 1/*C<sub>i</sub>* and 1/( $F_q'/F_m'$ ) or  $F_m'/F_q'$  gave a close linear relationship (Fig. 11B), so that *C<sub>i</sub>* could be determined from  $F_q'/F_m'$ . In all cases, the calibrations used were linear, reproducible, and *r*<sup>2</sup> values were >0.95. We assumed these relationships would hold constant whether a patch was present or absent. We verified that even after 10 to 15 min of exposure in some cases to low CO<sub>2</sub> concentration in the center of the patch combined with the low O<sub>2</sub> concentration, there were no changes in the *A* versus *C<sub>i</sub>* relationship that would otherwise invalidate our *C<sub>i</sub>* estimation procedure.

Using the CF imager software, parts of the  $F_q'/F_m'$  images with the patch and some surrounding leaf areas were isolated, smoothed using a loss-less, low-pass spatial filter, and the data transferred to Matlab (version 6.0 or 7.0; MathWorks). The calibration curve was then used to compute the *C<sub>i</sub>* value for each pixel. For comparison between conditions and with modeled results, average transects were calculated from three rows of pixels along the horizontal axis passing through the center of the patch image.

### Modeling Lateral Diffusion

Given the even light distribution used, the spatial pattern of *C<sub>i</sub>* under the patch depends on the effective lateral diffusion coefficient  $D_c'$ , the stomatal conductance to CO<sub>2</sub> (*g<sub>s</sub>'*) outside the patch, and the CO<sub>2</sub> assimilation rate, *A*, at different points along a distance from the boundary of the area being considered to the patch center. Since *A* is dependent on *C<sub>i</sub>* only (at constant light and temperature) and *C<sub>i</sub>* can be estimated from  $F_q'/F_m'$  using the calibration procedure (above), *A* can be determined at each point. As *g<sub>s</sub>'* may be measured (assumed constant over the whole surface), the main unknown is  $D_c'$ . A 2-D mathematical model was therefore developed by R. Herbin and E. Gallouët (Supplemental Appendix) to estimate  $D_c'$  and account for sinks and sources along the diffusion path. The 3-D diffusion equation was integrated over the depth of the leaf (the *z* dimension) to obtain a 2-D diffusion equation, the unknown of which is the value of *C<sub>i</sub>* averaged through the depth of the leaf. To do so, we approximate integrals in *z* by a one-point quadrature formula (for details, see Gallouët and Herbin, 2005). The resulting 2-D model

is equivalent to writing a balance equation for the diffusion fluxes in control volumes that run through the whole depth of the leaf replacing the point values of  $A$  and  $C_i$  by their mean value in the  $z$  direction (Supplemental Appendix). At the scale of the image pixels and the patches used here, we consider that treating the epidermis and stomata as simple porous boundaries, characterized by a conductance to CO<sub>2</sub> without details on stomatal size and distribution, is reasonable. The model used a hyperbolic function relating  $A$  to  $C_i$  ( $A = [(aC_i)/(b + C_i)] - c$ ) and used the finite volume method for the discretization of the diffusion equation (Eymard et al., 2000) considering fluxes in discrete radial segments centered on the middle of the patch.

A fixed point monotonic method was used to solve the resulting set of equations and compute  $C_i$  values for each discrete segment, and these were compared with the horizontal transects through the patch of fluorescence-derived  $C_i$  values (see above). An iterative procedure was then used to estimate the diffusion coefficient reduction factor ( $\phi$ ) value that produced the best fit between experimental and model values of  $C_i$ . The model was to analyze the experimental results; the sole fitted parameter was  $\phi$ , which was independently fitted to results at different  $C_a$  and for different leaves. Average values of  $\phi$  were computed for the two species examined from the different leaves. Further details of the model derivation and its fitting using Matlab version 6 are given in the Supplemental Appendix and in Gallouët (2004) and Gallouët and Herbin (2005).

## Leaf Sections

Sections taken from the middle part of the lamina were fixed overnight in glutaraldehyde (Agar Scientific) before being dehydrated by immersing them for 10 min each in a graded alcohol series (25%, 50%, 75%, 80%, 90%, and 100% ethanol). Following a second rinse in 100% ethanol, the sections were placed in 1:1 ethanol:LR White resin (London Resin) for 6 h. The sections were then placed in 100% LR White resin for several days, embedded in fresh resin in gelatin capsules, and polymerized overnight at 60°C. Thin transverse sections (10  $\mu$ m) were cut using an ultramicrotome, placed on microscope slides, and stained with 0.1% aqueous solution of toluidine blue (BDH). Measurements of leaf thickness, cell length, and air space as a fraction of total area (porosity) were made using image analysis software (ImageJ; National Institutes of Health) on images of sections from four leaves from different plants taken at  $\times 200$  magnification with a digital microscope camera.

## Stomatal Density

Stomatal density was determined in the midleaf lamina on four leaves of different plants for both the upper and lower epidermal surfaces. For *C. communis*, the lower or upper epidermis was peeled from the intact leaf and mounted onto a slide in water. Stomatal complexes in 4- $\times$  1-mm<sup>2</sup> areas were counted using a standard microscope at magnification of  $\times 200$ . For *P. vulgaris*, silicone rubber impressions were taken of the abaxial and adaxial leaf surfaces of four leaves with dental impression material (Xantropren VL plus; Heraeus Kulzer) according to the method of Weyers and Johansen (1985). The impressions were divided into two 10- $\times$  10-mm areas for each leaf, from which positives were made with clear nail varnish spread onto microscope slides. Stomatal numbers per area were counted in four fields of view following the systematic sampling strategy outlined by Poole and Kürschner (1999) using a microscope and eye piece graticule at  $\times 400$  magnification.

## ACKNOWLEDGMENTS

We are grateful to David Parkhurst (Indiana University) for his thorough review of the manuscript and many useful comments. T.L. was supported financially by the Department of Biological Sciences, University of Essex, during this research.

Received March 18, 2005; revised May 31, 2005; accepted June 1, 2005; published August 19, 2005.

## LITERATURE CITED

Aalto T, Juurola E (2002) A three-dimensional model of CO<sub>2</sub> transport in airspaces and mesophyll cells of a birch leaf. *Plant Cell Environ* **25**: 1399–1409

- Barbagallo RP, Oxborough K, Pallett KE, Baker NR (2003) Rapid, non-invasive screening for perturbations of metabolism and plant growth using chlorophyll fluorescence imaging. *Plant Physiol* **132**: 485–493
- Downton WJS, Loveys BR, Grant WJR (1988) Non-uniform stomatal closure induced by water stress causes putative non-stomatal inhibition of photosynthesis. *New Phytol* **110**: 503–509
- Esau K (1977) *Anatomy of Seed Plants*. John Wiley and Sons, New York
- Evans JR, Loreto F (2000) Acquisition and diffusion of CO<sub>2</sub> in higher plant leaves. In RC Leegood, TD Sharkey, S von Caemmerer, eds, *Photosynthesis: Physiology and Metabolism*. Kluwer Academic Publishers, Amsterdam, pp 321–351
- Evans JR, von Caemmerer SC (1996) Carbon dioxide diffusion inside leaves. *Plant Physiol* **110**: 339–346
- Eymard R, Gallouët T, Herbin R (2000) The finite volume method. In PG Ciarlet, JL Lions, eds, *Handbook for Numerical Analysis*, Vol VII. North-Holland, Amsterdam, pp 715–1022
- Gallouët E (2004) Diffusion of CO<sub>2</sub> in leaves. M.Sc. thesis. University of Paris, Paris
- Gallouët E, Herbin R (2005) Axisymmetric finite volumes for the numerical simulation of CO<sub>2</sub> transport and assimilation in a leaf. *Int J Finite Volumes* <http://averoes.math.univ-paris13.fr/JOURNAL/IJFV/index.php?name=Downloads&req=viewdownload&cid=1>
- Gillon JS, Yakir D (2000) Internal conductance of CO<sub>2</sub> diffusion and C<sup>18</sup>O discrimination in C<sub>3</sub> leaves. *Plant Physiol* **123**: 201–213
- Jahnke S, Krewitt M (2002) Atmospheric CO<sub>2</sub> concentration may directly affect leaf respiration measurement in tobacco, but not respiration itself. *Plant Cell Environ* **25**: 641–651
- Lawson T, James W, Weyers J (1998a) A surrogate measure of stomatal aperture. *J Exp Bot* **49**: 1397–1403
- Lawson T, Weyers J, A'Brook R (1998b) The nature of heterogeneity in the stomatal behaviour of *Phaseolus vulgaris* L. primary leaves. *J Exp Bot* **49**: 1387–1395
- Leuning R (1983) Transport of gases into leaves. *Plant Cell Environ* **6**: 181–194
- Long SP, Bernacchi CJ (2003) Gas exchange measurements, what can they tell us about the underlying limitations to photosynthesis? Procedures and sources of error. *J Exp Bot* **54**: 2393–2401
- Manter DK, Kerrigan J (2004) A/C<sub>i</sub> curve analysis across a range of woody plant species: influence of regression analysis parameters and mesophyll conductance. *J Exp Bot* **55**: 2581–2588
- Meyer S, Genty B (1998) Mapping intercellular CO<sub>2</sub> mole fraction (C<sub>i</sub>) in *Rosa rubiginosa* leaves fed with abscisic acid by using chlorophyll fluorescence imaging: significance of C<sub>i</sub> estimated from leaf gas exchange. *Plant Physiol* **116**: 947–957
- Morison JIL (1998) Stomatal response to increased CO<sub>2</sub> concentration. *J Exp Bot* **49**: 443–452
- Mott KA, Shope JC, Buckley TN (1999) Effects of humidity on light-induced stomatal opening: evidence for hydraulic coupling among stomata. *J Exp Bot* **50**: 1207–1213
- Pachepsky LB, Acock B (1996) A model 2DLEAF of leaf gas exchange: development, validation, and ecological application. *Ecol Model* **93**: 1–18
- Parkhurst DF (1977) A three dimensional model for CO<sub>2</sub> uptake by continuously distributed mesophyll in leaves. *J Theor Biol* **67**: 471–488
- Parkhurst DF (1986) Internal leaf structure: a 3-dimensional perspective. In TJ Givnish, ed, *On the Economy of Plant Form and Function*. Cambridge University Press, New York, pp 215–249
- Parkhurst DF (1994) Tansley Review 65: Diffusion of CO<sub>2</sub> and other gases inside leaves. *New Phytol* **126**: 449–479
- Parkhurst DF, Mott KA (1990) Intercellular diffusion limits to CO<sub>2</sub> uptake by leaves. *Plant Physiol* **94**: 1024–1032
- Parkhurst DF, Wong SC, Farquhar GD, Cowan IR (1988) Gradients of intercellular CO<sub>2</sub> levels across the leaf mesophyll. *Plant Physiol* **86**: 1032–1037
- Pieruschka R, Schurr U, Jahnke S (2005) Lateral gas diffusion inside leaves. *J Exp Bot* **56**: 857–864
- Pons TL, Welschen RAM (2002) Overestimation of respiration rates in commercially available clamp-on leaf chambers. Complications with measurement of net photosynthesis. *Plant Cell Environ* **25**: 1367–1372
- Poole I, Kürschner WM (1999) Stomatal density and index: the practice. In TP Jones, NP Rowe, eds, *Fossil Plants and Spores, Modern Techniques*. Geological Society, London, pp 257–260

- Singsaas EL, Ort DR, DeLucia EH** (2003) Elevated CO<sub>2</sub> effects on mesophyll conductance and its consequences for interpreting photosynthetic physiology. *Plant Cell Environ* **27**: 41–50
- Slaton MR, Smith WK** (2002) Mesophyll architecture and cell exposure to intercellular air space in alpine, desert, and forest species. *Int J Plant Sci* **163**: 937–948
- Syvertsen JP, Lloyd J, McConchie C, Kriedemann PE, Farquhar GD** (1995) On the relationship between leaf anatomy and CO<sub>2</sub> diffusion through the mesophyll of hypostomatous leaves. *Plant Cell Environ* **18**: 149–157
- Terashima I** (1992) Anatomy of non-uniform photosynthesis. *Photosynth Res* **31**: 195–212
- Terashima I, Ishibashi M, Ono K, Hikosaka K** (1996) Three resistances to CO<sub>2</sub> diffusion: leaf-surface water, intercellular space and mesophyll cells. In P Mathis, ed, *Photosynthesis: From Light to Biosphere: Proceedings of the Tenth International Photosynthesis Congress*. Kluwer Academic Publishers, Dordrecht, The Netherlands, pp 537–542
- Terashima I, Miyazawa SI, Hanba YT** (2001) Why are sun leaves thicker than shade leaves? Consideration based on analyses of CO<sub>2</sub> diffusion in the leaf. *J Plant Res* **114**: 93–105
- Terashima I, Wong SC, Osmond CB, Farquhar GD** (1988) Characterisation of non-uniform photosynthesis induced by abscisic acid in leaves having different mesophyll anatomies. *Plant Cell Physiol* **29**: 385–394
- von Caemmerer SC** (2003) C<sub>4</sub> photosynthesis in a single C<sub>3</sub> cell is theoretically inefficient but may ameliorate internal CO<sub>2</sub> diffusion limitations of C<sub>3</sub> leaves. *Plant Cell Environ* **26**: 1191–1197
- Warren CR** (2004) The photosynthetic limitation posed by internal conductance to CO<sub>2</sub> movement is increased by nutrient supply. *J Exp Bot* **55**: 2313–2321
- Weyers JDB, Johansen LG** (1985) Accurate estimation of stomatal aperture from silicone-rubber impressions. *New Phytol* **101**: 109–115
- Weyers JDB, Lawson T** (1997) Heterogeneity in stomatal characteristics. *Adv Bot Res* **26**: 317–351